Semiflexible Ribbon-Type Structures via Repetitive Diels-Alder Cycloaddition. Cage Formation versus Polymerization

M. Pollmann and K. Müllen*

Contribution from the Max-Planck-Institut für Polymerforschung, Ackermannweg 10, D-55128 Mainz, Germany

*Received June 14, 1993**

Abstract: Starting from various acetylenedicarboxylates (**1a–e**) as bis-dienophiles and [2.2](3,4)furanophane (**2**) as bis-diene, a series of ribbon-type oligomers (**6**) has been prepared via repetitive Diels–Alder reactions. Intramolecular Diels–Alder cycloaddition of **5**, the smallest "AB-type" building block of **6**, provides cage compound **7**, whose structure has been determined unambiguously by crystallography. In order to avoid competitive retro-Diels–Alder reactions, high-pressure conditions have been applied. This approach provides ribbon-type polymers which contain cyclooctadiene (COD) moieties as "semiflexible" units.

Introduction

Ribbon- or ladder-type structures consist of two parallel chains which are connected in a regular fashion via cross-links. If such two-dimensional structures contain reactive end groups, a polymerization or, alternatively, an intramolecular cyclization can occur. The latter process results in cage-type, so-called beltene, molecules which can function as hosts for small guest molecules.[1-3] The feasibility of a cyclization depends sensitively on the nature of the ribbon-type precursor, whereby a conformational flexibility of the repeating units is expected to be particularly important. If the ladder has a high degree of conformational freedom, then cage formation will proceed with low yields for entropic reasons; if the ladder is rigid, then cage formation can occur only in the case of an exact stereochemical fit of the building blocks. The latter process has been extensively discussed by Stoddard.[4]

Herein, we present ribbon structures containing cyclooctadiene (COD) units. COD can adopt a chair, a boat, and a twist-boat conformation.[5] It is relevant for our approach that these conformations differ in the distance of the double bonds and that a rapid conformational interconversion can occur in solution. A COD unit can therefore act as a "molecular hinge" within a ladder structure.

The method of choice for the synthesis of ladder-type molecules is the repetitive Diels–Alder reaction. The advantage of this polyaddition lies in the fact that even polymeric products can be prepared with high structural homogeneity.[6,7] In our approach toward "semiflexible" ribbon oligomers **6** (Scheme 1), the COD derivative furanophane **2** serves as bis-diene and acetylenedicarboxylate **1** as bis-dienophile. While **1** and **2** and their diadducts **3** and **4** constitute AA- and BB-monomers for a repetitive Diels–Alder reaction, the 1:1 adduct **5**, which contains both a diene and a dienophile function, constitutes an AB-type building block. Depending on which diene and dienophile are actually involved, one expects different pathways for the formation of the ribbon structures **6**.

Scheme 1. Building Blocks Used for the Diels–Alder Synthesis of Oligomers **6**[a]

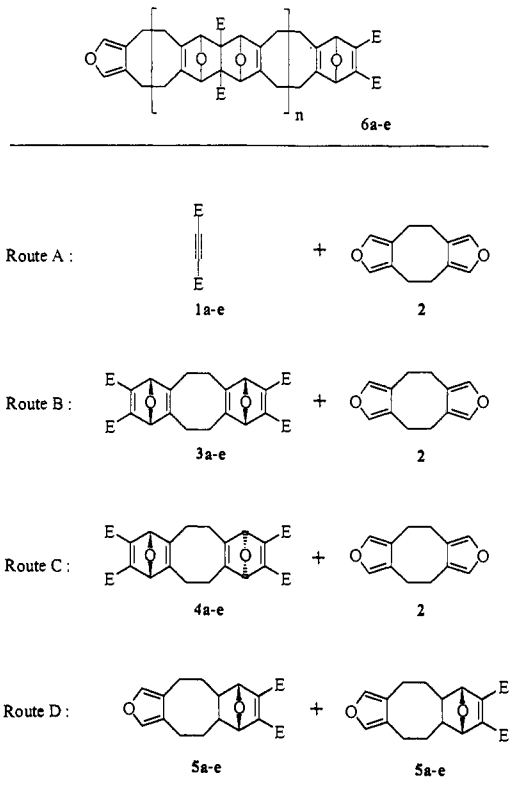

[a] **a**, E = COOMe; **b**, E = COOEt; **c**, E = COO^{t}Bu; **d**, E = $COOC_8H_{17}$; **e**, E = $COOC_2H_4OMe$.

It is also feasible that an intramolecular cycloaddition, under formation of cage compounds, competes with the intermolecular process. In rationalizing the product formation from **1** and **2**, we have simulated the structure and dynamics of ribbon-type structures **6** by the molecular modeling program SYBYL.[8]

Results and Discussion

Synthesis and Structural Description of Diels–Alder Building Blocks. A known procedure[9] has been scaled up so that [2.2](3,4)-furanophane (**2**) is now available on a 20-g scale. After sublimation, **2** is obtained as a pure, crystalline material.

* Abstract published in *Advance ACS Abstracts*, February 1, 1994.

(1) Stoddart, J. F.; Kohnke, F. H. *Angew. Chem., Int. Ed. Engl.* **1988**, *100*, 981.

(2) McMurry, J. E.; Harley, G. J.; Matz, J. R.; Clardy, J. C.; Mitchell, J. *J. Am. Chem. Soc.* **1986**, *108*, 515.

(3) Paquette, L. A.; Negri, J. T.; Rogers, R. D. *J. Org. Chem.* **1992**, *57*, 3947.

(4) Ashton, P. R.; Brown, G. R.; Isaacs, N. S.; Giuffrida, D.; Kohnke, F. H.; Mathias, J. P.; Slawin, A. M. Z.; Smith, D. R.; Williams, D. J.; Stoddart, J. F. *J. Am. Chem. Soc.* **1992**, *114*, 6330.

(5) Mackenzie, R. K.; MacNicol, D. D.; Mills, H. H.; Raphael, R. A.; Wilson, F. B.; Zabiewicz, I. A. *J. Chem. Soc., Perkin Trans.* **1972**, *2*, 1632.

(6) Schlüter, A. D. *Adv. Mater.* **1991**, *3*, 282.

(7) Bailey, W. J. In *Step Growth Polymerization*; Solomon, D. H., Ed.; Marcel Dekker Inc.: New York, 1972; p 2245.

(8) Version 5.4, available from TRIPOS Associates Inc.

(9) Garratt, P. J.; Neoh, S. B. *J. Org. Chem.* **1979**, *44*, 2667.

0002-7863/94/1516-2318$04.50/0

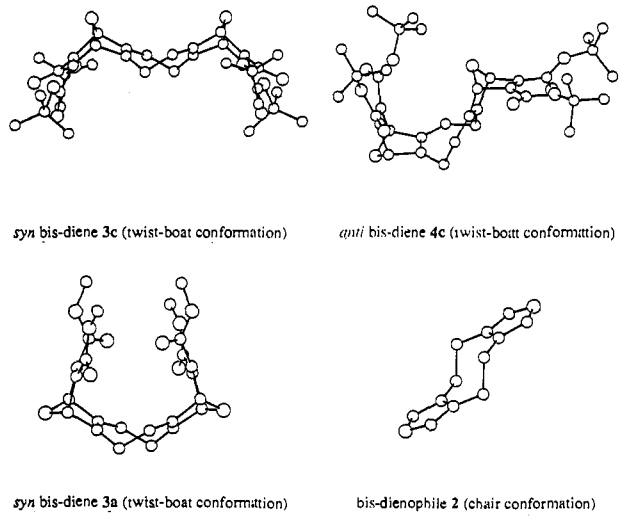

Figure 1. Crystal structures of **2**, **3a**, **3c**, and **4c**.

Addition of 1 equiv of acetylenedicarboxylate **1a** to 1 equiv of furanophane **2** in boiling THF affords, after 1 h, the AB-type momomer **5a**, which contains both a diene and a dienophile function. Attempted purification of **5a** by column chromatography gives rise to a polymerization of the material. This is obviously initiated by the Lewis acid activity of the silica gel. A similar finding has been made for the Diels–Alder reaction of norbornene-2,3-dicarboxylic anhydride with cyclopentadiene, which occurs only in the presence of silica gel.[10] We have avoided the column chromatography by synthesizing the octyl ester **5d**, which can be purified by extraction of the crude reaction product with pentane in 73% yield.

The Diels–Alder reaction of 2 equiv of acetylenedicarboxylate **1** with 1 eqiv of furanophane **2** during 2 h in boiling THF provides a 1:1 mixture of two diadducts which can be separated by fractional crystallization. The *syn* and *anti* configurations, **3** and **4**, respectively, of the oxygen bridges have been determined unambiguously by X-ray structural analysis of the isomers **3a** and **3c**,**4c** (see Figure 1) and then allowing for a ready ^{1}H NMR spectroscopic assignment via the typical AA'BB' spectra of their methylene protons.

The subsequent Diels–Alder reactions of **2**, **3**, **4**, and **5**, in particular the possibility of cage formation, depend sensitively on the conformation of the COD units. For the solid state, the different conformations are obvious from the crystal structures.

Furanophane **2**, which serves as an important model, has a COD unit with a chair conformation in the solid state. The conformation is probably stabilized by intermolecular π–π interactions of the aromatic furan moieties, leading to the formation of stacks.[11,12] In comparison to the boat conformation, there is a larger distance of 5.86 Å between the Diels–Alder reactive positions of the two furan groups which, in solution, should render an eventual cyclization more difficult. Upon a Diels–Alder cycloaddition, conformational change cannot be excluded.

The COD units of the isomeric diadducts **3c** and **4c** possess a twist-boat structure. One anticipates that an eventual cyclization starting from the anti isomer **4c** and a bis-diene (e.g. **2**) would result in cage compounds with a bulky oxygen bridge inside the cage and would certainly be less favorable than starting from the *syn* isomer **3c**. The steric repulsion of the *tert*-butyl ester groups of the diadducts **3c** and **4c** inhibits a closer approach of the dienophilic double bonds; thus, in the solid state, the *syn* isomer has a large distance of its dienophilic double bonds of 7.94 Å. In contrast to the *tert*-butyl ester-substituted **3c**, the methyl ester-substituted compound **3a** allows a smaller distance of the outer double bonds of 5.17 Å. We therefore expect the latter building block to be suitable for a cyclization.

The above structural description of the COD units applies to the solid state, while the COD unit should act as a *molecular hinge* in solution. We have therefore studied the dynamic behavior[13] of monomers **2** and **3c** by ^{1}H NMR spectroscopy (200 MHz) in solutions of CH_2BrF. The methylene protons of **2** give rise to a sharp singlet (δ 2.66) at room temperature pointing toward a rapid conformational interconversion. The slow-exchange domain of the ring inversion process is obtained at −100 °C, where the protons establish an AA'BB' spin system ($\Delta\nu$ = 124 Hz). Accordingly, if a chair conformation also prevails in solution, then there is a rapid ring inversion process. Since oligomers **6** contain no aromatic moieties such as furan, diadduct **3c** is probably a more appropriate model for **6**. This molecule exhibits a dynamic line broadening for which the slow-exchange domain is reached at −135 °C. While more detailled conformational analyses and a comparison of solution and solid-state structures are certainly beyond the scope of this text, it is clear that different conformations and thus different distances of the reactive groups are readily accessible.

The higher homologues of **6** are expected to exhibit a complicated conformational behavior due to the presence of many COD units. The particular conformations adopted will control the overall shape of the macromolecules. This situation will be simulated by a modeling program (see below).

Thermally Promoted Inter- and Intramolecular Diels-Alder Reactions. It appears that the Diels–Alder reaction between *tert*-butyl-substituted acetylenedicarboxylate (**1c**) and furanophane **2** is slow at 80 °C and that the resulting monoadduct **5c** and diadducts **3c** (*syn*) and **4c** (*anti*) are even less reactive. The low reactivity is due to the steric repulsion of the bulky *tert*-butyl groups; consequently, no *tert*-butyl ester-substituted monomers have been used for further reactions.

The less bulky 1:1 adduct **5a** (formed from methyl ester **1a** and **2**) readily undergoes subsequent cycloaddition, yielding 40% of oligomers **6a** via an intermolecular reaction and 20% of the compound **7a** (see Scheme 3) via an intramolecular reaction.

Oligomer **6a** has remaining end groups, allowing for the determination of its average number of repeating units by ^{1}H NMR spectroscopy: when comparing the relative signal intensities of the COD units and ester end groups of **6a**, the average number of repeating units is determined to be 2.5.

Compound **7a** has been isolated by column chromatography and characterized by ^{1}H and ^{13}C NMR spectroscopy (see Experimental Section). Evidence for a cage-type structure of compound **7a** comes from the missing end-group signals (furan and oxonorbornadiene). Since the cage structure of **7a** excludes a ring inversion, the AA'BB' spin system of the methylene protons is a most characteristic criterion within a ^{1}H NMR spectroscopic description of the title system.

In the case of compound **7e** (R = $C_2H_4OCH_3$), the cage-type structure has been determined unambiguously by X-ray crystallography (see Figure 2 and supplementary material), which also reveals the twist-boat conformation of the COD unit. Figure 2 shows that the ester groups and the two oxygen bridges of cage compound **7** are located outside the cage. This stereochemical outcome is in contrast to the known *endo rule*,[14] which is exemplified in Scheme 2. According to the *endo rule*, furan **9** approaches an oxonorbornadiene **8** only from the *oxygen face* of the latter. Two different routes are then feasible, leading to adducts **10** or **11**. No compound **12** is formed. If, however, **9**

(10) Bartlett, P. D.; Blakeney, A. J.; Kimura, M. K.; Warson, W. H. *J. Am. Chem. Soc.* **1980**, *102*, 1383.
(11) Jones, P. G. *Z. Naturforsch.* **1990**, *45b*, 1213.
(12) Baker, W.; Banks, R.; Lyon, D. R.; Mann, F. G. *J. Chem. Soc.* **1945**, *27*, 27.
(13) Paquette, L. A.; Kesselmayer, M. A.; Underiner, G. E.; House, S. D.; Rogers, R. D.; Meerholz, K.; Helnze, J. *J. Am. Chem. Soc.* **1992**, *114*, 2644.
(14) McCulloch, A. W.; Smith, D. G.; McInnes, A. G. *Can. J. Chem.* **1973**, *51*, 4125.

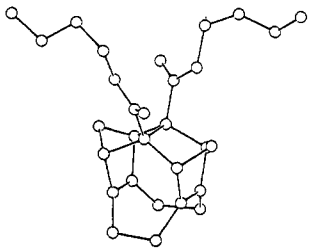

Figure 2. Crystal structure of cage compound **7e**.

Scheme 2. Inter- and Intramolecular Approaches of Furan (**9**) from the Oxygen Face of Oxonorbornadiene (**8**)

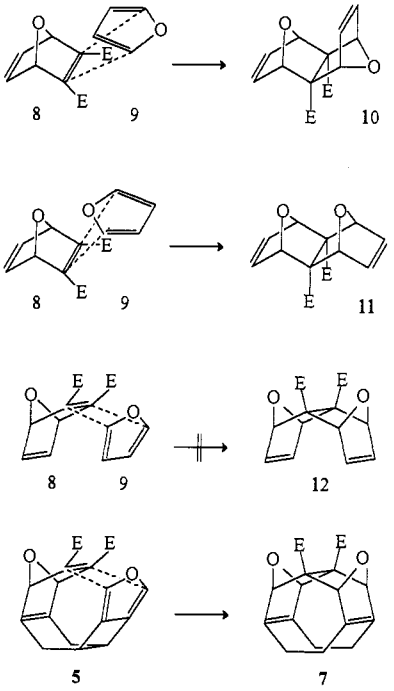

and **8** are linked via a COD unit, as in **5**, then the *exo* route is taken and cage compound **7** is formed.

The yields of cage compound **7**, amounting to 20%, can be improved by prolonged reaction times. This is due to the fact that the occurring oligomers **6**, but not **7**, undergo retro-Diels–Alder reactions. Therefore, cage precursor **5** is constantly produced from **6** via **13** and **14**, allowing for further cage formation. Evidence for this conclusion comes from the reaction of furanophane **2** and bis-dienophile **3a** which leads to cage compound **7a** (see Scheme 3). The "thermal" approach toward ribbon-type structures **6**, which also allows for a cyclization under formation of **7**, obviously has several disadvantages. Because of the low reactivity of the system of acetylenedicarboxylate **1a**/furanophane **2**, reaction temperatures of 80 °C are required. At this temperature the formation of oligomers **6** competes with the retro-Diels–Alder reaction of **6**. This equilibrium also excludes the formation of higher oligomers **6**. Indeed, larger cyclic oligomers have not been observed under these conditions. A further disadvantage of the thermal reaction is a partial thermal cleavage, leading to side products containing carboxyl groups which are detected by NMR and FT-IR. This can be ascribed to the appreciable strain occurring in the oxonorbornenes. Attempts to increase the molecular weights of oligomers **6a** by Lewis acid catalysis at room temperature have failed since the products are acid sensitive. In order to synthesize oligomers **6** with higher molecular weights and, eventually, larger cage compounds, we have focused on the high-pressure-promoted Diels–Alder reactions.

Diels–Alder Reactions under High Pressure. It is well established for Diels–Alder reactions of furans that high-pressure

Scheme 3. Competitive Formation of Linear Structures **6** and Cage Compound **7** (see Route C of Scheme 1) as Affected by the Retro-Diels–Alder Reaction[a]

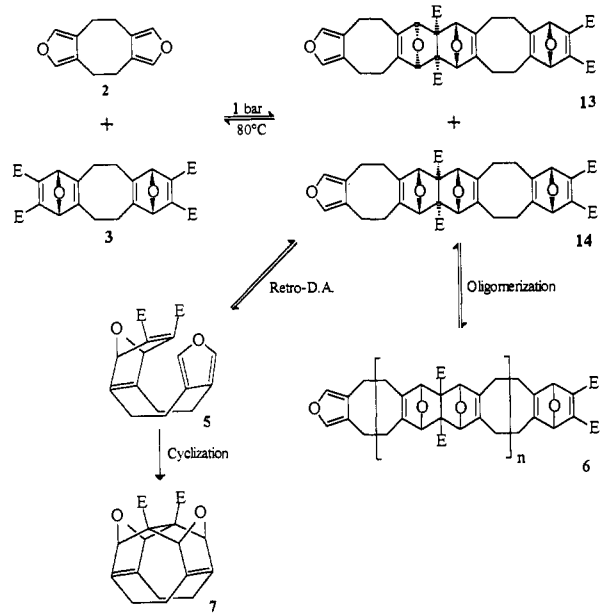

[a] **a**, E = COOMe; **b**, E = COOEt; **c**, E = COO^{t}Bu; **d**, E = COOC$_8$H$_{17}$; **e**; E = COOC$_2$H$_4$OMe.

conditions (7-10 kbar)[15,16] increase the rate constants by a factor of 10-1000 and shift equilibria toward the Diels–Alder adducts.[17] We have investigated this method (see Scheme 1) for polymerization and cyclization via routes A (**1a**,**e** with **2**), B (**3a**,**d** with **2**), and C (**5d**,**e** with **5d**,**e**). The reaction conditions and results of these experiments are summarized in Table 1.

The crude polymer **6e** (experiment 4) has been purified by precipitation in MeOH. The average degree of polymerization, $\bar{P}_n$, has been determined by ^{1}H NMR end-group analysis and by gel permeation chromatography (GPC). Based on polystyrene standards, GPC elugram of **6e** shows an average molecular weight (M_n) of 5130 g/mol. Based on the ribbon-type molecule **3** as standard, the resulting M_n = 7690 g/mol, and $\bar{P}_n$ = 9.5 appears to be in accordance with ^{1}H NMR spectroscopic data ($\bar{P}_n$ = 11).

The following findings (see Table 1) emerge from the high-pressure reactions.

(i) Higher Degree of Polymerization ($\bar{P}_n$) of 6. In contrast to the thermal conditions (experiment 1), high-pressure conditions result in polymers **6a** with an increased $\bar{P}_n$ ($\bar{P}_n$ = 10 instead of 2.5). The reaction proceeds smoothly until no monomer is left (experiment 2, 0.1 mol/L; 80 °C; 8000 bar; 2 days).

If monomer **1a** is replaced by the larger monomer **3** (experiment 7), then fewer addition steps are required to attain a higher molecular weight; not surprisingly, therefore, polymers **6** with a $\bar{P}_n$ of 27 are now available.

The degree of polymerization strongly depends on a sufficient solubility of the products (e.g., using octyl ester groups). Under high-pressure conditions, solubility is generally reduced,[15] and oligomeric products may precipitate, thus limiting $\bar{P}_n$. Additionally, precipitation will cause a deviation from an exact 1:1 stoichiometry of the reacting species which is also essential for a high $\bar{P}_n$. When using higher monomer concentrations (experiment 3, 0.18 mol/L), precipitation obviously results in a low degree of polymerization ($\bar{P}_n$ = 8), since the moderately soluble furanophane **2** (0.22 M at ambient pressure) precipitates. This problem can be avoided, however, by using an AB-type monomer

(15) LeNoble, W. J. *Organic High Pressure Chemistry* Elsevier: New York, 1988; Vol. 37, pp 154–155.
(16) Dauben, W. G.; Krabbenhoft, H. O. *J. Am. Chem. Soc.* **1976**, *98*, 1992.
(17) Klärner, F. G. *Chem.-Ztg.* **1989**, *23*, 53.

Table 1. Experimental Conditions and Yields for the Investigated Diels–Alder Reactions

							cage compounds		oligomers **6**	
expt no.	route[a]	COOR, R	conc [mol/L]	temp [°C]	pressure [bar]	time [day]	compd	yield [%]	$\bar{P}_n$	yield [%]
1	A	Me	0.1	80	1	2	**7a**	20	2.5	40
2	A	Me	0.1	80	8000	2	**7a**	23	10	77
3	A	C_2H_4OMe	0.18	30	8000	12	**7e**	10	8	10
4	A	C_2H_4OMe	0.1	90	8000	2	**7e**	55	11	45
5	B	C_2H_4OMe	0.6	100	6500	3	**7e**	60	25	40
6	B	Octyl	0.1	50	8000	1	**7d**	20	17	80
7	C	Octyl	0.05	50	8600	5	**15d**	54	27	46
8	C	Me	0.1	50	7000	0.5	**15a**	46	18	54

[a] Route A, acetylenedicarboxylate **1** + furanophane **2**. Route B, monoadduct **5** + monoadduct **5**. Route C, furanophane **2** + *syn* diadduct **3**.

5. Now the monomer concentration can be increased (experiment 5, 0.6 mol/L), resulting in a $\bar{P}_n$ of 25 instead of 17 (experiment 6, 0.1 mol/L).

(ii) Improved Yields. Since the conversion is quantitative under high-pressure conditions, larger amounts of products **6** and **7** (experiment 2, 77% and 23%, respectively) become available. The yields of cage compound **7**, however, are not influenced by high pressure. This is remarkable because intramolecular reactions have been described to be favored by high-pressure conditions.[18,19] The increasing tendency toward cyclization is reported to be due to a higher solvent viscosity at high pressure, which protects a reactive species from undergoing an intermolecular reaction.[20]

(iii) Fewer Side Reactions. No structural defects have been observed in polymer **6** by IR and NMR analysis (see Experimental Section). In accordance, the crude reaction mixture is colorless, while in the case of the thermal reaction at ambient pressure, the crude product is yellow.

(iv) Controllable Size and Yield of Cage Compounds. Using routes A and B (see Scheme 1), oligomers **6** and exclusively cage compound **7** occur. Noncyclized oligomers **6** are favored by low temperatures (experiment 6, 50 °C; 80% of **6**); cage compound **7** is favored by higher temperatures (experiment 5, 100 °C; 60% of **7**).

When using route C (see Scheme 1), no cage compound **7** but oligomers **6** and an additional product are formed. The structural description of the latter is discussed below.

Detection of Cage Compounds. If the hydrodynamic volumes of the cage compounds differ sufficiently from those of their open-chain precursors, GPC serves as an appropriate method for detecting cage compounds. Indeed, in the case of cage compound **7** we have observed a bimodal elugram (one peak for **7** and one broad peak for the oligomers **6**). This method fails, however, if the hydrodynamic volumes of the cage and its precursor are similar. This may explain why we cannot detect larger cage compounds by GPC.

NMR spectroscopy reveals that 50% of ribbon-type polymer **6**, containing up to 27 repeating units, and 50% of a second product are formed upon high-pressure reaction of bis-dienophile **3** and furanophane **2** (experiments 7 and 8). Attempted purification of the second product by column chromatography (Al_2O_3, SiO_2) gives rise to decomposition. A structural elucidation of this product by spectroscopic means has therefore only been performed for a sample with 90% purity. The ^1H NMR spectrum (see Figure 3 and supplementary material) can be divided into four parts: the signals of bridgehead protons (4.16 ppm, H-3, 4 H, s; 4.87 ppm, H-5, 4 H, s), those of methoxy groups (3.68 ppm, H-9, 12 H, s), and those of two different COD units (2.85–2.10 ppm, H-1, 8 H, AA'BB', 2.38 ppm, H-7, 8 H, br s).

There are no signals of end groups, indicating that the compound is a macropolycycle rather than a linear ribbon oligomer.

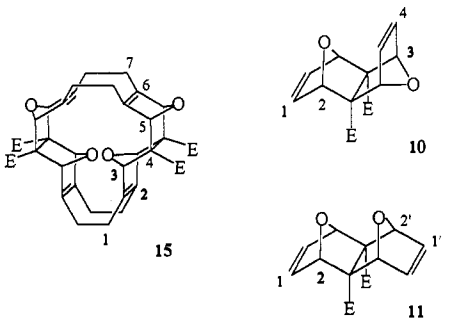

Figure 3. Structure of cage compound **15** and model compounds **10** and **11**.

Comparison of the spectral data of the bridgehead protons with those of model compounds **10** and **11** (see Scheme 2) (^1H NMR δ 5.17 (H-5, 2 H), 4.52 (H-3, 2 H), and 5.07 (H-3, 4 H)) strongly suggests an *anti* geometry of the two oxygen atoms. Furthermore, the detection of only nine ^{13}C NMR signals (see Experimental Section) points toward a high symmetry. From the above pieces of evidence, we tentatively assign structure **15a** to the second product.

Model considerations leave no doubt that the ester groups must be located outside the cage. An unambiguous structure determination of **15a** would require an X-ray analysis. Unfortunately, single crystals of **15a** have not been obtained due to the presence of small amounts of **6a** in the crude material. Furthermore, handling of **15a** is difficult because it undergoes a retro-Diels–Alder reaction in solution. This reaction is accelerated on silica gel. The cleavage of the cage in solution (at 21 °C) has been monitored by ^1H NMR spectroscopy. Analysis of the increasing intensity of furan signals points toward a zero-order reaction with a half-life time τ of 261 h.

Relative Stabilities of the Cage Compounds and Dynamics of Ribbon Structures 6. In order to further elucidate the conditions under which a ribbon-type oligomer **6** can undergo a cyclization, we have utilized a program package which allows the calculation of larger molecular geometries. Firstly, we examined whether the molecular geometries of **3a**, **3c**, **4c**, and **7e**, as obtained by crystal structure analysis, can be reproduced by the molecular modeling programs INSIGHT[21] or SYBYL.[22] Only the program SYBYL (version 5.4) provides structures in good agreement with the experimental ones, so all further modeling has been performed by SYBYL. Based on the calculated geometries of cage compounds **7** and **15** and of the elusive compound **16** (Scheme 4) as well as those of the linear ribbon compounds **5** and **13**, the corresponding enthalpies of formation, ΔH_f, have been determined. Since the applied AM1 Hamiltonian[23] is limited to 102 atoms, larger molecules such as **14a** and **13a** have been treated as the corresponding aldehydes (indicated by *) rather than as the alkyl esters. The data are collected in Table 2.

(18) Isaacs, N. S.; van der Beeke, P. *Tetrahedron Lett.* **1982**, *23*, 2147.
(19) Vögtle F. *Topics in Current Chemistry: Macrocycles*; Springer Verlag: Berlin, 1992; Vol. 161, p 28.
(20) Iurczak, I.; Ostazewski, R.; Salanski P. *J. Chem. Soc., Chem. Commun.* **1989**, 184.
(21) Dauber-Osguthorpe, P.; Roberts, V. A.; Osguthorpe, D. J.; Wolff, J.; Genest, M.; Hagler, A. T. *Proteins: Struct. Funct. Genet.* **1988**, *4*, 31.
(22) Clark, M.; Cramer, R. D.; VanOpdenbosch, N. *J. Comput. Chem.* **1989**, *10*, 982.
(23) Dewar, M. J. S.; Zoebisch, E. G.; Healy, E. F.; Steward, J. J. P. *J. Am. Chem. Soc.* **1985**, *107*, 3903.

Scheme 4. Calculated Changes of Enthalpies of Formation, $\Delta\Delta H_f$ [kcal/mol], for Different Reactions of AB-Monomer **4**

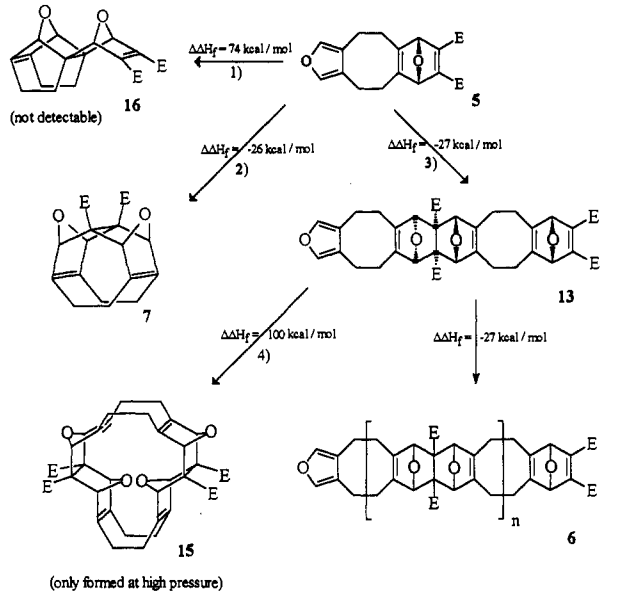

Table 2. Calculated Enthalpies of Formation ΔH_f, of Several Intermediates

molecule[a]	ΔH_f(calcd) (kcal/mol)
5a	−67
7a	−93
16a	8
5*	30
15*	106
13*	6

[a] **a**, E = COOMe; *, E = CHO.

The high ΔH_f values of cage compounds **16a** and **15***, in contrast to those of cage compounds **7a** and **7***, clearly indicate a higher stability of the latter. This is in accordance with both the failure to experimentally detect compound **16a** and the tendency of **15a**, containing the highly strained body of compound **15***, to undergo a retro-Diels–Alder reaction at ambient pressure.

For a more detailed view, we have focused on the changes of enthalpies of formation, $\Delta\Delta H_f$, as occurring upon different reactions of AB-type molecule **5** (see Scheme 4).

Comparing the $\Delta\Delta H_f$ values of reaction pathways 1 and 2, according to Scheme 4, the cyclization of **5a** to **7a** ($\Delta\Delta H_f$ = −26 kcal) is exothermic, while the formation of the highly strained cage compound **16a** ($\Delta\Delta H_f$ = 74 kcal) is endothermic, and this nicely reproduces the experimental findings. The competing pathway 3 is the dimerization of **5a** to the ribbon-type molecule **13** ($\Delta\Delta H_f$ = −27 kcal), which then further transforms into oligomers **6**. Oligomer **13** itself can, in principle, undergo a subsequent addition of a molecule **5** or an intramolecular cyclization toward **15** (pathway 4). While the $\Delta\Delta H_f$ for the former process is approximately −27 kcal/mol, the formation of **15** is highly endothermic ($\Delta\Delta H_f$ = −100 kcal/mol). In agreement with the lower stability of **15** in comparison to cage compound **7**, this cage compound has not been obtained at ambient pressure and is stable only under high-pressure conditions.

The thermodynamic arguments based on the AM1 calculations thus rationalize satisfactorily the product spectrum observed when starting from **5**. What remains unclear is why under high-pressure conditions the strained cage compound **15** but not cage compound **16** can be detected. Kinetic considerations, thereby assuming that the AB-monomer **5** reacts much faster toward **7** than toward **16**, could, of course, be involved as well. In order to obtain a model for the oligomers **6** and their eventual cyclization, one arbitrary isomer of the numerous isomers of a heptamer **6** has been constructed by SYBYL using the geometries of **3** and **4**, as obtained by crystal structure analyses. Due to the large number of atoms, all ester groups have been replaced by hydrogens. The dynamic during 100 ps of heptamer **6** has been simulated for 1000 K, and 100 conformations have been examined. It is remarkable that most of the conformations of heptamer **6** show a small distance of the end groups (about 2 nm, see Figure 4). The "bent" shape of heptamer **6** should, in principle, allow for a cyclization and nicely supports the role of the COD moieties as *molecular hinges*. All moieties of ribbon-type heptamer **6** maintain a plane of symmetry, and the mobility of heptamer **6** is confined to two dimensions. The ends of this ribbon-type structure are constrained to exist only within this mirror plane (see Figure 5). A similar finding has been made for other ribbon-type oligomers.[24,25]

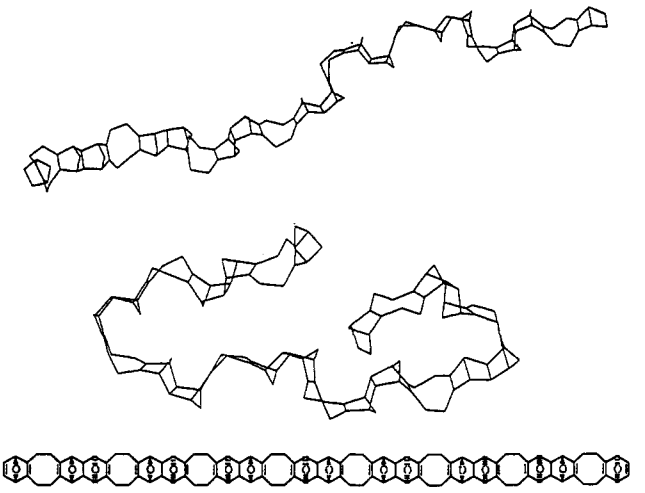

Figure 4. "Stretched" (top) and "bent" (bottom) shape of heptamer **6**, determined by a dynamic simulation. "Head-to-tail" distances: stretched, 4.9 nm; bent, 0.5 nm.

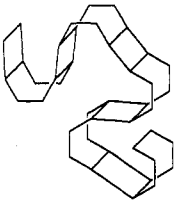

Figure 5. Part of ribbon-type heptamer **6** in simplified representation.

Conclusion.

By using repetitive Diels–Alder reactions, novel ribbon-type oligomers **6** have been synthesized. In agreement with dynamic simulations (SYBYL), their COD units act as *molecular hinges* and lead to intramolecular cyclizations in addition to the formation of extended ribbon-type structures. Not surprisingly, therefore, the concave shape of **5a** allows for the synthesis of the novel cage compound **7a** in good yields (50%) without using high dilution. Under high-pressure conditions, extended ribbon-type structures **6** with about 25 repeating units and the highly strained cage compound **15a** have been obtained. Investigations concerning the detection and isolation of cage compounds larger than **15a** are still in progress.

Experimental Section

General. Melting points are uncorrected. ^{1}H NMR spectra were recorded at 200 MHz, ^{13}C NMR spectra at 50 MHz, in $CDCl_3$. Liquid chromatography was performed on Merck silica gel 60 (230–400 mesh).

(24) Schürmann, B. L.; Enkelmann, V.; Löffler, M.; Schlüter A.-D. *Angew. Chem., Int. Ed. Engl.* **1993**, *105*, 981.
(25) Sastri, V. R.; Schulman, R.; Roberts, D. C. *Macromolecules* **1982**, *15*, 939.

Table 3. Crystallographic Data for **2**, **3a**, **3c**, **4c**, and **7e**[a]

	2	3a	3c	4c	7e
formula	$C_{12}H_{12}O_2$	$C_{24}H_{24}O_{10}$	$C_{36}H_{48}O_{10}$	$C_{36}H_{48}O_{10}$	$C_{22}H_{22}O_8$
fw	188.23	472.45	640.77	640.77	418.20
T [K]	298	298	298	298	293
a [Å]	6.9596(7)	18.928(4)	11.668(1)	14.497(4)	27.5380(3)
b [Å]	12.3211(8)	9.717(2)	28.667(2)	16.853(1)	12.5900(7)
c [Å]	11.1317(8)	15.537(3)	10.551(8)	14.569(1)	11.3439(6)
β [deg]		129.50(2)		91.71(1)	91.926(8)
V [Å^3]	954.6(2)	2858(1)	3529(2)	3558(1)	3934(2)
d_c [g/cm^3]	1.31	1.423	1.21	1.20	1.413
Z	4	4	4	4	8
space group	*Pbca*	*C*2/*c*	*Iba*2	$P2_1/c$	*C*2/*c*
radiation	Cu Kα	Mo Kα	Cu Kα	Cu Kα	Cu Kα
reflctns	505	1311	749	3972	1867
R	0.047	0.051	0.044	0.062	0.065
R_w	0.047	0.055	0.042	0.060	0.051

[a] **a**, E = COOMe; **c**, E = COO^{t}Bu; **e**, E = $COOC_2H_4OMe$.

[2.2](3,4)Furanophane (2). Bis(3-propyne) ether (100 g, 1.06 mol) in 400 mL of THF was slowly added to a boiling solution of KO^{t}Bu (70 g, 0.62 mol) in 1.5 L of THF. The strongly exothermic reaction resulted in an orange-red solution, which was concentrated under reduced pressure and partitioned between water and CH_2Cl_2. The combined organic layers were washed with water and dried (Na_2SO_4). Removal of the solvent under reduced pressure provided a viscous oil. After addition of 50 mL of cold acetone, the resulting precipitate was filtered to give 16 g (16% yield) of crystalline furanophane **2**: mp 170 °C; ^{1}H NMR (200 MHz, $CDCl_3$) δ 7.12 (4 H, s), 2.66 (8 H, s); ^{13}C NMR (50 MHz, $CDCl_3$, DEPT) δ (C) 125.66, (CH) 139.96, (CH_2) 24.92. Crystallographic data are provided in Table 3 and the supplementary material.

***Syn* Diadduct 3a.** Furanophane **2** (1.88 g, 20 mmol) and DMAD (**1a**) (6.4 g, 45 mmol) were heated to reflux in 20 mL of THF for 2 h. The mixture was cooled to 4 °C, and the precipitate was filtered off. Pure *syn* diadduct **3a** was obtained (5.18 g, 49%): mp 171 °C; ^{1}H NMR (200 MHz, $CDCl_3$) δ 5.24 (4 H, s), 3.78 (12 H, s), 2.61 (8 H, AA'BB'); ^{13}C NMR (50 MHz, $CDCl_3$, DEPT) δ (C) 163.25, 152.38, 146.93, (CH) 90.08, (CH_2) 25.59, (CH_3) 51.95.

***Anti* diadduct 4a** was obtained by fractional crystallization of the remaining mother liquor at about −15 °C. The product was isolated as an amorphous powder (4.97 g, 47%): mp 128 °C; ^{1}H NMR (200 MHz, $CDCl_3$) δ 5.24 (4 H, s), 3.78 (12 H, s), 2.57 (8 H, AA'BB'); ^{13}C NMR (50 MHz, $CDCl_3$, DEPT) δ (C) 163.50, 152.61, 147.16, (CH) 89.83, (CH_2) 25.52, (CH_3) 52.15.

AB-Monomer 5d. Dioctyl acetylenedicarboxylate (**1d**) (1.69 g, 5 mmol) in 5 mL of THF was slowly added to a solution of furanophane **2** (1.88 g, 5 mmol) in 20 mL of boiling THF using a pressure-equalizing funnel. After 1 h the solvent was removed under reduced pressure, and the remaining oil was extracted with water/pentane. The colorless **5d** (2.36 g, 88%) was obtained: ^{1}H NMR (200 MHz, $CDCl_3$) δ 7.05 (2 H, s), 5.26 (2 H, s), 4.16 (4 H, t), 2.98–2.50 (8 H, ABCD), 1.70 (20 H, q), 0.91 (6 H, t); ^{13}C NMR (50 MHz, $CDCl_3$, DEPT) δ (C) 163.2, 152.84, 147.19, 124.21, (CH) 140.19, 90.82, (CH_2) 65.89, 32.24, 29.68, 29.64, 29.28, 29.06, 26.37, 23.09, 22.29, (CH_3) 14.50; EI m/z (relative intensity) 526 (M^+, 5), 396 (M − $COOC_8H_{17}$, 11%), 255 (M − 2 $COOC_8H_{17}$, 13%), 188.

AB-Monomer 5e. Bis(methoxyethyl) acetylenedicarboxylate (**1e**) (1,7 g, 5 mmol) in 5 mL of THF was slowly added to a solution of furanophane **2** (1.88 g, 5 mmol) in 20 mL of boiling THF. After 1 h the solvent was removed under reduced pressure, and the remaining oil was purified by column chromatography (silica gel, CH_2Cl_2:THF = 10:1, R_f = 0.83). The product obtained solidified slowly at low temperatures (648 mg, 31%): ^{1}H NMR (200 MHz, $CDCl_3$) δ 7.08 (2 H, s), 5.27 (2 H, s), 4.28 (4 H, m), 3.62 (4 H, t), 3.34 (4 H, s), 298–2.50 (8 H, ABCD); ^{13}C NMR (50 MHz, $CDCl_3$, DEPT) δ (C) 164.02, 153.83, 148.03, 125.21, (CH) 140.95, 91.25, (CH_2) 71.15, 65.07, 29.73, 22.67, (CH_3) 59.15.

Oligomers 6a (Methyl Ester Groups). A solution of furanophane **2** (564 mg, 3 mmol) and **3a** (1417 mg, 3 mmol) in 20 mL of CH_2Cl_2 was heated in a sealed poly(tetrafluoroethylene) (PTFE) tube to 50 °C at 7 kbar for 12 h. ^{1}H NMR spectroscopic analysis revealed a 46% yield of cage compound **15a** and a 54% yield of **6a** with an average degree of polymerization of 18: ^{1}H NMR (200 MHz, $CDCl_3$) δ 7.12 (2 H, s, end group, furan), 5.28 (2 H, s, end group, oxonorbornadiene), 3.77 (6 H, s, end group, methyl ester), 3.65/3.55 (chain, methyl ester), 4.80/4.16 and 4.63 (chain, bridge position), 2.05–3.00 (br m, chain, cyclooctadiene units); ^{13}C NMR (50 MHz, $CDCl_3$, DEPT) δ (C) 173 (chain, CO), 164 (end group, oxonorbornadiene CO), 153/147/146 (end group, oxonorbornadiene), 124 (end grop, furan), 69 (chain), (CH) 140 (end group, furan), 90–89/85–84 (chain), (CH_2) 28–22 (chain, cyclooctadiene units), (CH_3) 52 (chain, methyl ester).

Cage Compound 7a. A solution of furanophane **2** (0.8 g, 4.2 mmol) and DMAD (**1a**) (600 mg, 4.2 mmol) in 20 mL of CH_2Cl_2 was heated in a sealed PTFE tube to 90 °C at 8 kbar for 40 h. Cage compound **7a** was isolated by precipitation in CH_2Cl_2/Et_2O. Subsequent column chromatography (silica gel, $CHCl_3$, R_f = 0.67) provided pure **7a** (0.71 g, 51% yield) as a colorless powder: ^{1}H NMR (200 MHz, $CDCl_3$) δ 4.84 (4 H, s), 3.78 (6 H, s), 2.60–2.10 (8 H, AA'BB'); ^{13}C NMR (50 MHz, $CDCl_3$, DEPT) δ (C) 173.73, 141.02, 72.12, (CH) 88.48, (CH_2) 21.03, (CH_3) 53.45. Anal. Calcd for $C_{18}H_{18}O_6$: C, 65.45; H, 5.49; O, 29.06. Found: C, 65.21; H, 5.46; O, 29.33.

Cage Compound 7e. A solution of furanophane **2** (0.8 g, 4.2 mmol) and bis(methoxy ethyl) acetylenedicarboxylate (**1e**) (966 mg, 4.2 mmol) in 20 mL of CH_2Cl_2 was heated in a sealed PTFE tube to 90 °C at 8 kbar for 40 h. Cage compound **7e** was isolated by precipitation in CH_2Cl_2/Et_2O (0.89 g, 50% yield) as a colorless powder: ^{1}H NMR (200 MHz, $CDCl_3$) δ 4.88 (4 H, s), 4.36 (4 H, m), 3.66 (4 H, m), 3.39 (6 H, t), 2.70–2.08 (8 H, AA'BB'); ^{13}C NMR (50 MHz, $CDCl_3$, DEPT) δ (C) 172.96, 141.83, 72.08, (CH) 88.36, (CH_2) 70.73, 65.14, 20.87, (CH_3) 59.41. Anal. Calcd for $C_{22}H_{22}O_8$: C, 63.75; H, 5.35; O, 30.99. Found: C, 63.17; H, 5.31; O, 31.52.

Cage Compound 15a. A solution of furanophane **2** (941 mg, 5 mmol) and diadduct **3a** (2362 mg, 5 mmol) in 20 mL of CH_2Cl_2 was heated in a sealed PTFE tube to 50 °C at 7 kbar for 12 h. The yield of cage compound **15a**, as determined by ^{1}H NMR spectroscopy, was 46%. **15a** could be enriched to 90% by extracting the solid product mixture with THF: ^{1}H NMR (200 MHz, $CDCl_3$) 4.87 (4 H, s), 4.16 (4 H, s), 3.68 (12 H, s), 2.85–2.10 (8 H, AA'BB'), 2.38 (8 H, br s); ^{13}C NMR (50 MHz, $CDCl_3$, DEPT) δ (C) 173.03, 146.67, 138.88, 69.06, (CH) 89.71, 84.66, (CH_2) 27.30, 25.07, (CH_3) 52.63; FD-MS M^+ = 626.2 g/mol.

Crystal Structure of 2, 3a, 3c, 4c, 7e (Table 3). Single crystals were obtained from sublimation (**2**) and from CH_2Cl_2–Et_2O at 5 °C. Intensity data were collected on an Enraf-Nonius CAD-4 diffractometer to an I limit of 55° in 2θ mode. The structures were solved by using the direct methods program MULTAN and refinement with the full-matrix least-squares method. Positional and anisotropic thermal parameters were refined without the hydrogen atoms, except for **3a**.

Acknowledgment. Financial support by the Bundesministerium für Forschung und Technologie and by the Fonds der Chemischen Industrie is gratefully acknowledged.

Supplementary Material Available: X-ray coordinates and thermal parameters for **2**, **3a**, **3c**, **4c**, and **7e**; AM1 calculations of **5**, **5a**, **7a**, **13**, **15**, and **16a**; and selected mass and NMR spectra (55 pages); listing of observed and calculated structure factors for **2**, **3a**, **3c**, and **4c** (52 pages). This material is contained in many libraries on microfiche, immediately follows this article in the microfilm version of the journal, and can be ordered from the ACS; see any current masthead page for ordering information.